Sensitive Magnetometry based on Nonlinear Magneto-Optical Rotation

D. Budker[1,2,*], D. F. Kimball[1], S. M. Rochester[1], V. V. Yashchuk[1], and M. Zolotorev[3]
[1] *Department of Physics, University of California at Berkeley, Berkeley, California 94720-7300*
[2] *Nuclear Science Division, Lawrence Berkeley National Laboratory, Berkeley, California 94720*
[3] *Center for Beam Physics, Lawrence Berkeley National Laboratory, Berkeley, California 94720*
(Received:)

Application of nonlinear magneto-optical (Faraday) rotation to magnetometry is investigated. Our experimental setup consists of a modulation polarimeter which measures rotation of the polarization plane of a laser beam resonant with transitions in Rb. Rb vapor is contained in an evacuated cell with antirelaxation coating which enables atomic ground state polarization to survive many thousand wall collisions. This leads to ultranarrow features ($\sim 10^{-6}$ G) in the magnetic field dependence of optical rotation. The potential sensitivity of this scheme to sub-μG magnetic fields as a function of atomic density, light intensity, and light frequency is investigated near the D1 and D2 lines of ^{85}Rb. It is shown that through an appropriate choice of parameters the shot-noise-limited sensitivity to small magnetic fields can reach 3×10^{-12} G/$\sqrt{\text{Hz}}$.

PACS. 07.55.Ge, 32.80.Bx, 42.50.Gy

I. INTRODUCTION

Optical pumping magnetometers [1,2] have achieved sensitivities of $\approx 3 \times 10^{-11}$ G/$\sqrt{\text{Hz}}$ (see, e.g., [3,4] and references therein). There is considerable interest in improving the sensitivity of magnetic field measurements both for practical applications and for fundamental research. For example, sensitive magnetometry and related techniques are applied in tests of discrete symmetries in atomic systems [5,6]. Atomic magnetometers based on nonlinear magneto-optical (Faraday) rotation (NMOR) [7,8] may be able to enhance sensitivity to magnetic fields compared to conventional optical pumping magnetometers [9]. In this work we show that NMOR with ultranarrow linewidths ($\sim 2\pi\times 1$ Hz, demonstrated in [10,11]), achieved by employing an evacuated alkali vapor cell with high quality paraffin coating [3], can in principle be used to reach a shot-noise-limited sensitivity of $\approx 3 \times 10^{-12}$ G/$\sqrt{\text{Hz}}$. We perform a systematic investigation of the shot-noise-limited sensitivity to magnetic fields with respect to light intensity, light frequency, and atomic density. It is demonstrated that the sensitivity can be considerably improved by detuning light from the center of a Doppler-broadened absorption profile [12]. It is interesting to note that the optimum sensitivity in this experiment is close to the shot-noise limit for an ideal experiment with the given number of atoms in the vapor cell ($\sim 10^{12}$ at room temperature ≈ 20 ^{o}C) and rate of ground state relaxation, demonstrating the high efficiency of NMOR-based magnetometry.

Faraday rotation is a process in which the plane of light polarization rotates as light propagates through a medium along the direction of a magnetic field. Typically, in the case of resonant atomic media, there are several nested, dispersively-shaped features of different widths in the magnetic field dependence of the rotation (see, e.g., Ref. [13] and references therein). For example, there is a linear Faraday rotation feature [14] with a width determined by Doppler broadening. This feature arises because the Zeeman splitting of magnetic sublevels shifts the resonance frequencies for right- and left-circularly polarized light. There are also nonlinear Faraday rotation features, such as the Bennett structure-related feature which has a width determined by the lifetime of the excited state (see, e.g., Ref. [8] and references therein). The narrowest features in the magnetic field dependence of the Faraday rotation are due to NMOR associated with light-induced ground state polarization (coherence effects). The Bennett-structure and coherence effects are nonlinear in the sense that they require at least two light-atom interactions, one to prepare the atomic sample (e.g., optical pumping [15]) and a second interaction to probe the atomic sample. Because magnetometry based on the Faraday effects employs detection of forward-scattered light, it can be much more efficient than schemes based on fluorescence detection [16].

The sensitivity δB_z to magnetic fields along the direction of light propagation ($\hat{z}$) is given by:

$$\delta B_z = \left(\frac{\partial\varphi}{\partial B_z}\right)^{-1} \delta\varphi, \tag{1}$$

where $\delta\varphi$ is the sensitivity to light polarization rotation (measured in, e.g., rad·Hz$^{-1/2}$ [18]) and $\partial\varphi/\partial B_z$ is the slope of the optical rotation with respect to a longitudinal magnetic field B_z. The shot-noise limit of $\delta\varphi$ is inversely proportional to the square root of the transmitted light power [19]. Assuming that transverse fields are compensated at a level much smaller than the value of B_z where optical rotation reaches a maximum (which ensures that the B_z-dependence of NMOR has a dispersive shape [10]), for magnetic field sensitivity near $B_z = 0$ we have:

$$\delta B_z \approx \frac{1}{\sqrt{P}}\left(\frac{\partial\varphi}{\partial B_z}\right)^{-1} \propto \frac{1}{\sqrt{P}}\left(\frac{\gamma_{\text{rel}}}{\varphi_{\max}}\right), \tag{2}$$

where P is the light flux transmitted through the cell in photons per second, γ_{rel} is the relevant effective relax-

ation rate, and $\varphi_{\max}$ is the maximum rotation angle with respect to magnetic field.

When applied to the coherence effects in NMOR, which are related to the evolution of light-induced atomic polarization, Eq. (2) indicates that decreasing the relaxation rate of atomic ground state polarization can improve the sensitivity to magnetic fields. In our experiment, we obtain ultranarrow NMOR resonances in the coherence effects [10] by using evacuated vapor cells with high quality paraffin coating [3]. The depolarization rate limits the amount of time that polarized atoms can evolve in the magnetic field before probing. Since atoms can undergo many thousand collisions with the paraffin-coated cell walls without depolarizing, in our case the upper limit on the average precession time ($\sim$ 350 ms at 20 ^{o}C) is determined by relaxation due to spin-exchange collisions. Although our apparatus is not currently shot noise limited, by measuring $\partial\varphi/\partial B_z$ and the transmitted light intensity we can estimate the shot-noise-limited sensitivity using Eq. (2).

II. EXPERIMENTAL SETUP

In this work, we investigate coherence effects in nonlinear Faraday rotation for the D1 and D2 lines of ^{85}Rb (Fig. 1). The experimental apparatus (Fig. 2) for these measurements is essentially the same as that used in our previous experiments [10,11]. We use tunable external cavity diode lasers to produce light at 795 nm for the D1 line ($^2S_{1/2} \rightarrow {}^2P_{1/2}$) and 780 nm for the D2 line ($^2S_{1/2} \rightarrow {}^2P_{3/2}$). Frequency of the D1 laser is monitored by observing fluorescence from an additional uncoated Rb vapor cell and the signal from a confocal Fabry-Perot spectrum analyzer [13]. Frequency of the D2 laser is monitored by observing the signals from the Fabry-Perot cavity and a DAVLL (dichroic atomic vapor laser lock) [20,21]. These signals permit relative frequency calibration of NMOR spectra to within $\approx$ 10 MHz (laser linewidths are $\leq$ 7 MHz). Before entering the antirelaxation coated Rb vapor cell (10 cm diameter), the light passes through an attenuator (used to adjust light intensity), a linear polarizer, and a Faraday rotator (for calibration of rotation angles). The coated vapor cell is inside a four-layer magnetic shield which provides nearly isotropic shielding of external dc magnetic fields at a level of 1 part in 10^6 [11]. Residual magnetic fields are compensated to less than 0.1 μG (averaged over the cell volume) by three mutually perpendicular magnetic coils using the techniques of 3-axis magnetometry discussed in Refs. [10,11]. At room temperature (20^{o}C) the atomic number density is $\approx 4.5 \times 10^9$ cm^{-3}, which corresponds to on the order of one absorption length at the center of resonance lines. For investigation of magnetometer sensitivity with respect to atomic density, the vapor cell is heated to around 30^{o}C by channeling warm air into the inner magnetic shield. The atomic density is determined from fits of the light transmission spectrum to a Voigt profile.

NMOR signals are detected using the technique of modulation polarimetry (see, e.g., Ref. [22]). After passing through the coated Rb vapor cell, light goes through a second Faraday rotator which modulates the direction of linear polarization at a frequency of 1 kHz with a 5 mrad amplitude. The polarization of the light is subsequently analyzed with a polarizing beam splitter aligned with the initial light polarization. The first harmonic of the signal from the photodiode PD1, which detects light from the nearly-crossed channel of the polarizing beamsplitter, is measured with a lock-in amplifier. Transmitted light intensity is the sum of the light detected with the bright channel (PD2) and the dark channel (PD1) of the analyzer. The ratio of the first harmonic signal from PD1 to the transmitted light intensity is a measure of the optical rotation angle [22].

III. LIGHT FREQUENCY DEPENDENCE OF COHERENCE EFFECTS IN NMOR

In order to optimize the sensitivity of an NMOR-based magnetometer, it is essential to understand the dependence of optical rotation on experimental parameters, such as light frequency. There are a variety of physical mechanisms which determine the spectra of NMOR for the coherence effects. When atomic polarization survives many wall collisions between pumping and probing (the wall-induced Ramsey effect [23], Fig. 3), atoms which are optically pumped in a particular resonant velocity group generally return to the beam with a different velocity. In the case where Doppler-broadened hyperfine transitions overlap, it is possible for the light to be resonant with different transitions during pumping and probing. For example, when the laser is tuned to the center of the $F_g = 3$ component of the D1 line (see Fig. 4(a)), an atom pumped on the $F_g = 3 \rightarrow F_e = 2$ transition can be probed with comparable probability on either the $F_g = 3 \rightarrow F_e = 3$ or the $F_g = 3 \rightarrow F_e = 2$ transition, where F_g and F_e are the total angular momenta of the ground and excited states, respectively. The same is true for atoms pumped on the $F_g = 3 \rightarrow F_e = 3$ transition. Atoms pumped on $F \rightarrow F$ and $F \rightarrow F - 1$ transitions tend to populate different ground state sublevels, and the dark state for an $F \rightarrow F$ transition is a bright state for an $F \rightarrow F - 1$ transition. Similarly, the dark state for an $F \rightarrow F - 1$ transition is a bright state for an $F \rightarrow F$ transition. Consequently, for $F \rightarrow F, F - 1$ transitions, the contribution to optical rotation from atoms pumped and probed on different transitions is of opposite sign compared to the contribution from atoms pumped and probed on the same transition. In this case, the wall-induced Ramsey rotation spectrum consists of two peaks, since the contributions to optical rotation nearly cancel at the center of the Doppler profile.

This can be contrasted with a situation where the relaxation of ground state polarization is determined by

the time of flight of atoms through the light beam (the transit effect, Fig. 3). Here atoms remain in a particular resonant velocity group (in the absence of velocity-changing collisions) during optical pumping and probing. Therefore the contributions to rotation from each velocity group add near the center of the Doppler profile (Fig. 4(b)).

It has also recently been observed that AC Stark shifts of the ground state sublevels caused by the electric field of the light can significantly modify NMOR spectra [24]. At light powers where the number of optical pumping cycles during the relaxation time of ground state coherences exceeds unity, ground state alignment [25] created by optical pumping can be efficiently converted into orientation via the combined action of the magnetic field and the optical electric field [26–30]. This effect leads, for example, to a change in the overall sign of rotation for closed $F \rightarrow F+1$ transitions as light power is increased.

In the following, we focus on nonlinear Faraday rotation for the hyperfine transitions which exhibit the largest optical rotation for the wall-induced Ramsey effect: the $F_g = 3 \rightarrow F_e = 2, 3, 4$ component of the D2 line and the $F_g = 3 \rightarrow F_e = 2, 3$ component of the D1 line, respectively (Fig. 1).

IV. SENSITIVITY AS A FUNCTION OF LIGHT FREQUENCY AND INTENSITY

The spectra of $\partial\varphi/\partial B_z$ for the $F_g = 3$ components of the D1 and D2 lines are shown in Figs. 5(a) and 6(a), respectively. Figures 5(b) and 6(b) show light transmission through the cell, where incident light intensities for the D1 and D2 lines are 1 mW/cm^2 and 4.5 mW/cm^2, respectively (beam diameter ≈ 3 mm). The optimum shot-noise-limited sensitivity is obtained for these light intensities, as discussed below. The slopes were determined by taking the difference of nonlinear Faraday rotation spectra with $B_z = \pm 1$ μG, which cancels magnetic-field-independent background rotation. The primary contribution to the background rotation has a spectral and light intensity dependence similar to that of self-rotation of elliptical polarization [17]. The magnitude of the effect is consistent with that expected from self-rotation induced by residual elliptical polarization of the incident light (which is nominally linearly polarized) due to the non-ideality of the polarizers and birefringence of the vapor cell wall.

From the measurements of $\partial\varphi/\partial B_z$ and transmitted light intensity, the shot-noise-limited sensitivity δB_z to longitudinal magnetic fields can be found using Eq. (2). The sensitivity as a function of light detuning from the center of the Doppler-broadened $F_g = 3$ components of the D1 and D2 lines is shown in Figs. 5(c) and 6(c). Note that for both the D1 and D2 lines, the sensitivity can be improved by detuning the light from the center of the Doppler-broadened resonance. In fact, detuning the light improves the sensitivity over the entire range of light powers studied (although the frequency where the optimum sensitivity is achieved is observed to change slightly with light power).

The sensitivity as a function of light intensity is shown in Fig. 7. The optimal value δB_z with respect to laser frequency and intensity is:

$$\delta B_z \approx 3 \times 10^{-12} \text{ G}/\sqrt{\text{Hz}}.$$

This is a factor of 8 improvement from our previous result [11,18], obtained without systematic optimization. This optimum sensitivity is achieved at a laser intensity ≥ 4.5 mW/cm^2 and frequency tuned ≈ 0.4 GHz to the high frequency side of the $F_g = 3$ component of the D2 line. The optimum sensitivity for the D1 transition is $\delta B_z \approx 4 \times 10^{-12}$ G/$\sqrt{\text{Hz}}$ at a laser intensity of ≈ 1 mW/cm^2 with frequency tuned ≈ 0.6 GHz to the low frequency side of the $F_g = 3$ component.

We believe that the difference in the light intensities where optimum sensitivity occurs for the D1 and D2 lines is related to the saturation behavior of the hyperfine transitions involved. At the frequencies where optimum sensitivity is achieved, the primary contribution to optical rotation for the D1 line is from the open $F_g = 3 \rightarrow F_e = 2$ transition and for the D2 line, the closed $F_g = 3 \rightarrow F_e = 4$ transition. Specifically, in contrast to the $F_g = 3 \rightarrow F_e = 2$ D1 transition, the $F_g = 3 \rightarrow F_e = 4$ D2 transition has no dark state and is a cycling transition. Thus significant differences in saturation behavior occur for these two cases. It should also be noted that at the light powers where highest sensitivity is obtained, alignment-to-orientation conversion is expected to be a dominant mechanism in NMOR [24].

V. SENSITIVITY AS A FUNCTION OF ATOMIC DENSITY

Our approach to NMOR-based magnetometry [10,11] takes advantage of the ultranarrow linewidths in the wall-induced Ramsey effect obtained with evacuated, antirelaxation coated cells. Another technique to achieve narrow NMOR resonances employs cells with buffer gas to increase the transit time of atoms through the laser beam [31]. Under conditions of relatively high atomic density ($\sim 10^{12}$ atoms/cm^3) and high light intensities (~ 25 mW/cm^2), it has been shown that shot-noise-limited sensitivities surpassing $\approx 10^{-10}$ G/$\sqrt{\text{Hz}}$ are possible with this approach [31]. It is suggested that by increasing atomic density and light power, NMOR-based magnetometer sensitivity can be further improved (as in the case of the recently proposed, closely related phaseonium magnetometer [32]).

We have investigated the dependence of sensitivity on atomic number density at a relatively high laser intensity (20 mW/cm^2) for the D2 line (Fig. 8). The sensitivity

was studied over a range of densities between 4.5 and 14 $\times 10^9$ cm^{-3}, corresponding to cell temperatures of 20 to 30^{o}C, limited by our present thermal stabilization system. The atomic densities were determined by fits to the absorption profiles at low light intensity. Over this range of densities we do not find a significant change in δB_z.

The behavior of δB_z with respect to density can be understood as follows. With the laser frequency detuned from the center of the absorption profile at the high light intensity used, there is little absorption over the entire range of densities studied. Therefore the transmitted light power P is independent of density, so the shot-noise-limited sensitivity $\delta\varphi$ to rotation angle is constant. At the light intensities and detunings where optimum sensitivity is achieved for each density, the relaxation rate due to spin-exchange collisions $\gamma_{\rm se}$ is greater than or comparable to the light broadening rate $\gamma_{\rm light}$ [10,11]. Under these conditions, the sensitivity δB_z is approximately independent of atomic density since both $\varphi_{\rm max}$ and $\gamma_{\rm rel} \sim \gamma_{\rm se}$ are proportional to atomic density (Eq. (2)).

VI. ADDITIONAL CONSIDERATIONS

As discussed in Refs. [33,10,11], transverse magnetic fields (e.g., B_x) can also be detected with the present apparatus. We find experimentally that if the transverse fields are compensated to a level well below $|B_z^{\rm max}|$ they do not significantly affect sensitivity to longitudinal fields. This is because near $B_z = 0$, if the transverse magnetic fields are much less than $|B_z^{\rm max}|$, the nonlinear Faraday rotation is linear with respect to longitudinal magnetic field while there is a quadratic dependence of rotation on transverse fields (the nonlinear Voigt effect, see e.g., Refs. [34,35]). The amplitude of the transverse magnetic field where optical rotation due to the nonlinear Voigt effect reaches a maximum is approximately $|B_z^{\rm max}|$.

Optimization of an NMOR magnetometer also involves the choice of the atom. In order to employ the paraffin coating to achieve low spin-relaxation rates, the stable isotopes of sodium, potassium, rubidium, and cesium (among the alkali atoms) are most convenient; for these species, sufficient atomic densities are achieved in the range of temperatures for which the paraffin coating works. We plan to investigate NMOR for different species of atoms in the future.

There is also a question of the optimum laser beam diameter. Our present apparatus limits the range over which the beam diameter can be varied to a few mm. No significant change in sensitivity was observed over this range. Estimates indicate that the sensitivity cannot be improved by more than a factor of 2-3 (if at all) by changing the laser beam diameter, although we plan to investigate this question more carefully with density matrix calculations in the near future. We have also recently investigated NMOR with Rb in paraffin-coated cells using two spatially separated laser fields [36]. Such a scheme offers the possibility of independent optimization of the light frequency and intensity of both pump and probe.

Recent experiments have indicated a promising new way to obtain ultranarrow resonances [37]. When alkali atoms contained in vapor cells filled with He buffer gas are cooled below $\sim$ 2K, the cross-sections for spin-exchange relaxation reportedly decrease by orders of magnitude. In principle, this may allow $\gamma_{\rm rel}$ to reach the mHz range and correspondingly improve the sensitivity of NMOR-based magnetometry.

VII. CONCLUSION

In conclusion, we have conducted a systematic study of the shot-noise-limited sensitivity of a magnetometer based on nonlinear magneto-optical rotation with respect to light frequency, light intensity, and atomic density. We find that by optimizing an NMOR-based magnetometer with respect to these parameters, a shot-noise-limited sensitivity of 3×10^{-12} G/$\sqrt{\rm Hz}$ is achievable. If limitations due to technical sources of noise can be overcome, the sensitivity of an NMOR-based magnetometer may be able to surpass that of current optical pumping [3–5] and SQUID (superconducting quantum interference device) magnetometers [38] (both of which operate near their shot-noise-limit) by an order of magnitude. It is interesting to note that this sensitivity to magnetic fields corresponds to a sensitivity of 10^{-6} Hz/$\sqrt{\rm Hz}$ to atomic energy level shifts, indicating that the general techniques employed may be of considerable interest for a variety of fundamental and practical applications.

The results of our present investigation may be useful in the development of an NMOR-based magnetometer for use in the Earth field range ($|B| \sim 0.5$ G) and the application of closely related nonlinear electro-optic effects (NEOE) to precise electric field measurements [39]. We also hope to apply similar methods in a search for a permanent electric dipole moment (EDM) [8,40,10,11,41]. The optimum shot-noise-limited sensitivity to the EDM should occur under parameters close to those where an NMOR-based magnetometer reaches optimum sensitivity to magnetic fields (see, e.g., Ref. [11]).

ACKNOWLEDGMENTS

The authors are grateful to E. B. Alexandrov, A. I. Okunevich, and D. DeMille for helpful discussions. We would also like to thank S. Siu for valuable assistance, and A. Vaynberg and M. Solarz for help in construction of the experimental apparatus. This research has been supported by the Office of Naval Research (grant N00014-97-1-0214) and by the U.S. Department of Energy through the LBNL Nuclear Science Division (Contract No. DE-AC03-76SF00098).

* e-mail: budker@socrates.berkeley.edu

[1] E.B. Alexandrov, A.M. Bonch-Bruevich, and V.A. Khodovi, Opt. Spectrosk. **23**, 282 (1967) (Opt. Spectrosc. (USSR), **23**, 151 (1967)).

[2] J. Dupont-Roc, S. Haroche and C. Cohen-Tannoudji, Phys. Lett. **28A**, 638 (1969); C. Cohen-Tannoudji, J. Dupont-Roc, S. Haroche, and F. Laloe, Phys. Rev. Lett. **22**, 758 (1969).

[3] E.B. Alexandrov, M.V. Balabas, A.S. Pasgalev, A.K. Vershovskii, and N.N. Yakobson, Laser Phys. **6**, 244 (1996).

[4] E. B. Alexandrov and V. A. Bonch-Bruevich, Opt. Engin. **31**, 711 (1992).

[5] L.R. Hunter, Science **252**, 73 (1991).

[6] I.B. Khriplovich and S.K. Lamoreaux, *CP Violation Without Strangeness* (Springer-Verlag, Berlin, 1997).

[7] A review of earlier work on NMOR is given by: W. Gawlik, in *Modern Nonlinear Optics* edited by M. Evans and S. Kielich, Advances in Chemical Physics Series, Vol. **LXXXV**, Pt. 3 (Wiley, New York, 1994).

[8] L. M. Barkov, M. S. Zolotorev and D. Melik-Pashayev, Sov. JETP Pis'ma **48**, 144 (1988); Opt. Commun. **70**, 467 (1989).

[9] There is an important distinction between optical pumping magnetometers such as the Hanlé type [2], which measure only weak fields within the range of the Hanlé linewidth, and magnetometers using magnetic resonance [3], which measure the absolute value of the magnetic field over a wide range of field strengths. In this paper, we specifically consider the sensitivity of an NMOR magnetometer of the former type, but it appears possible to apply similar methods to construct an NMOR-based magnetometer having the advantages of the latter type [D. Budker, D.F. Kimball, and V.V. Yashchuk, Report LBNL PUB-5449 (1999), to be published].

[10] D. Budker, V. Yashchuk, and M. Zolotorev, Phys. Rev. Lett. **81**, 5788 (1998).

[11] V. Yashchuk, D. Budker and M. Zolotorev, in *Trapped Charged Particles and Fundamental Physics*, edited by D.H.E. Dubin and D. Schneider (American Institute of Physics, New York, 1999), pp. 177-181.

[12] Advantages of detuning the light frequency from resonance were discussed earlier in the context of optical pumping magnetometers in: E. B. Alexandrov, M. V. Balabas, and V. A. Bonch-Bruevich, Sov. Tech. Phys. Lett. **13**, 312 (1987) (Pis'ma Zh. Tekh. Fiz. **13**, 749 (1987)). In that experiment there were separate light sources for pumping and probing, and only the dependence of sensitivity on probe light detuning was discussed.

[13] D. Budker, D. J. Orlando, and V. Yashchuk, Am. J. Phys. **67**, (1999); D. Budker, V. Yashchuk, and M. Zolotorev, Sib. J. Phys. **1**, 27 (1999).

[14] D. Macaluso and O.M. Corbino, Nuovo Cim. **8**, 257 (1898).

[15] W. Happer, Rev. Mod. Phys. **44**, 169 (1972).

[16] It has also been noted [A.I. Okunevich, private communications] that, in comparison to resonance magnetometers employing circular polarization for optical pumping and monitoring the frequency of RF-induced transitions [3], the use of linearly polarized light in NMOR-based magnetometry reduces the systematic error in magnetic field measurements due to light shifts between Zeeman sublevels. In the case of NMOR, systematic error due to light shifts arises only due to residual ellipticity of the nominally linearly polarized incident light, in which case the major axis of the polarization ellipse can undergo self-rotation (see, e.g., Ref. [17] and references therein). Due to the fact that self-rotation and NMOR have distinct spectral dependences, proper choice of laser frequency may be able to virtually eliminate systematic error arising from light shifts in an NMOR-based magnetometer.

[17] D. Budker, R. Y. Chiao, D. S. Hsiung, S. M. Rochester, and V. V. Yashchuk, *Technical Digest of Conference on Lasers and Electro-Optics, Quantum Electronics and Laser Science*, 252 (2000); R.Y. Chiao, J. Bowie, J. Boyce, D. Budker, J.C. Garrison, M.W. Mitchell, V. Yashchuk, T.K. Gustafson, and D.S. Hsiung, *Technical Digest of Conference on Lasers and Electro-Optics, Quantum Electronics and Laser Science*, 259 (1999).

[18] The relationships between the sensitivity for a measurement time of 1 s and sensitivity per unit bandwidth depends on the spectral characteristics of the experimental setup. In the literature, one finds several relationships, including $G \cdot \sqrt{s} \rightarrow G/\sqrt{Hz}$ (e.g. [11]), $G \cdot \sqrt{s} \rightarrow G/\sqrt{Hz} \cdot \sqrt{\pi}$, $G \cdot \sqrt{s} \rightarrow G/\sqrt{Hz} \cdot 2$, and $G \cdot \sqrt{s} \rightarrow G/\sqrt{Hz} \cdot \sqrt{2\pi}$ [E. B. Alexandrov and J. Clarke, private communications]. Here we present results assuming $G \cdot \sqrt{s} \rightarrow G/\sqrt{Hz} \cdot \sqrt{\pi}$.

[19] Note, however, that with squeezed states of light the sensitivity to polarization rotation can in principle surpass the shot-noise-limit: see, e.g., P. Grangier, R.E. Slusher, B. Yurke and A. LaPorta, Phys. Rev. Lett. **59**, 2153 (1987).

[20] K.L. Corwin, Z.-T. Lu, and C.E. Wieman, Appl. Opt. **37**, 3295 (1998).

[21] V.V. Yashchuk, D. Budker, and J.R. Davis, Rev. Sci. Instr. **71**(2), 341 (2000).

[22] G.N. Birich, Yu.V. Bogdanov, S.I. Kanorskii, I.I. Sobelman, V.N. Sorokin, I.I. Struk, and E.A. Yukov, J. of Russian Laser Research, **15**, 455 (1994).

[23] S. I. Kanorsky, A. Weis and J. Skalla, Appl. Phys. B, **60**, S165 (1995).

[24] D. Budker, D.F. Kimball, S.M. Rochester, and V.V. Yashchuk, Report LBNL-45259 (2000), to be published.

[25] There are different definitions of the terms "alignment" and "orientation" in the literature. For example, in R. N. Zare, *Angular Momentum* (John Wiley & Sons, New York, 1988), alignment designates even moments in atomic polarization (quadrupole, hexadecapole, etc.), while orientation designates the odd moments (dipole, octupole, etc.). We use the convention employed in E. B. Alexandrov, M. P. Chaika, and G. I. Kvostenko, *Interference of Atomic States* (Springer-Verlag, Berlin, 1993), where alignment designates the second (quadrupole) po-

larization moment, and orientation designates the first (dipole) polarization moment.
[26] M. Lombardi, J. Physique **30**, 631 (1969).
[27] C. Cohen-Tannoudji and J. Dupont-Roc, Opt. Commun. **1**, 184 (1969).
[28] M. Pinard and C.G. Aminoff, J. Physique **43**, 1327 (1982).
[29] R.C. Hilborn, L.R. Hunter, K. Johnson, S.K. Peck, A. Spencer, and J. Watson, Phys. Rev. A **50**, 2467 (1994).
[30] R.C. Hilborn, Am. J. Phys. **63**, 330 (1995).
[31] V.A. Sautenkov, M.D. Lukin, C.J. Bednar, G.R. Welch, M. Fleischhauer, V.L. Velichansky, and M.O. Scully, quant-ph/9904032 (1999); M. Fleischhauer, A.B. Matsko, and M.O. Scully, Phys. Rev. A **62**, 013808 (2000).
[32] M. Fleischhauer and M. O. Scully, Phys. Rev. A **49**, 1973 (1994); H. Lee, M. Fleischhauer, and M. O. Scully, Phys. Rev. A **58**, 2587 (1998).
[33] D. Budker, V. Yashchuk, and M. Zolotorev, in *Proceedings of ICAP XVI: Abstracts of Contributed Papers* (University of Windsor, Windsor, 1998).
[34] K.H. Drake, W. Lange and J. Mlynek, Opt. Commun. **66**, 315 (1988).
[35] X. Chen, V.L. Telegdi, and A. Weis, Opt. Commun. **78**, 337 (1990).
[36] V.V. Yashchuk, E. Mikhailov, I. Novikova, and D. Budker, Report LBNL-44762, (1999).
[37] A. Hatakeyama, K. Oe, K. Ota, S. Hara, J. Arai, T. Yabuzaki, and A.R. Young, Phys. Rev. Lett. **84**, 1407 (2000).
[38] J. Clarke in *The New Superconducting Electronics*, edited by H. Weinstock and R.W. Ralston, pp. 123-180 (Kluwer Academic, The Netherlands, 1993).
[39] Since the density of atomic vapor in the evacuated cells near room temperature corresponds to high vacuum conditions, it is in fact possible to apply reasonably large electric fields without the use of a buffer gas.
[40] B. Schuh, S. I. Kanorsky, A. Weis, and T.W. Hansch, Opt. Commun. **100**, 451 (1993)
[41] Application of *linear* electro-optic rotation to the search for EDMs was first considered in N.B. Baranova, Yu. V. Bogdanov, and B. Ya. Zel'dovich, Sov. Phys. Usp. **20**, 870 (1977), and O.P. Sushkov and V.V. Flambaum, Sov. JETP **75**, 1208 (1978).

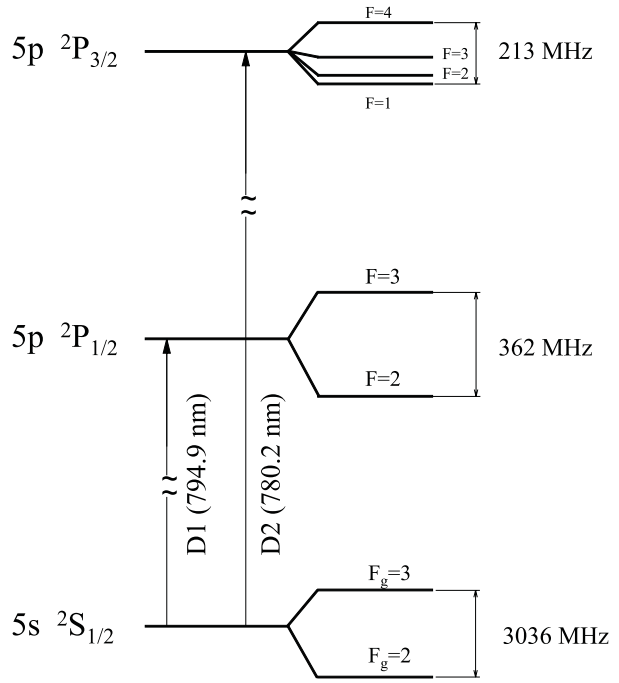

FIG. 1. Partial energy level diagram of ^{85}Rb (nuclear spin = 5/2) with hyperfine splittings and relevant transitions (not to scale).

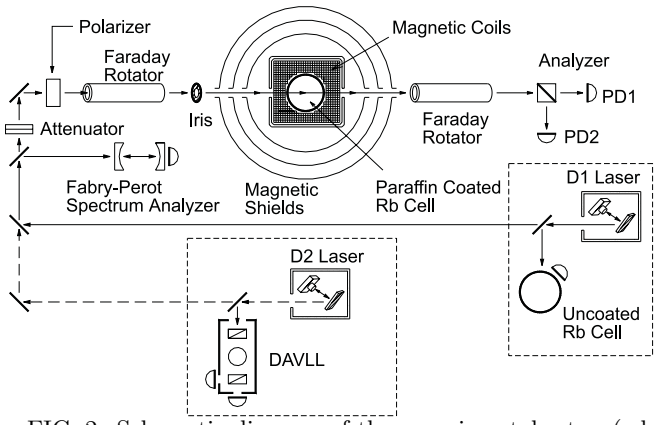

FIG. 2. Schematic diagram of the experimental setup (additional electronic elements are described in [10,11]).

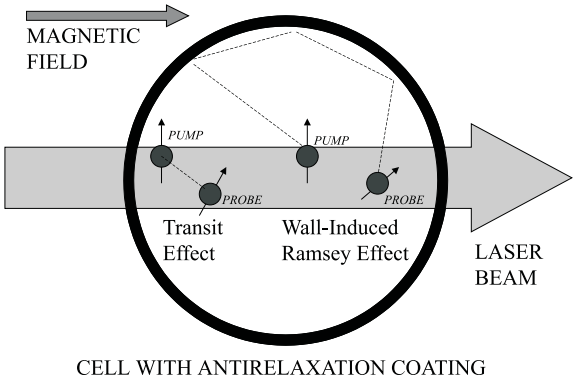

FIG. 3. Illustration of the transit and wall-induced Ramsey effects in a cell with antirelaxation coating. The linearly polarized light induces ground state polarization which evolves in the longitudinal magnetic field. The evolution of atomic polarization can both cause the atomic vapor to acquire circular birefringence [24] and rotate the axis of linear dichroism with respect to the initial plane of light polarization [10,11], causing optical rotation as light propagates through the vapor. In the transit effect, pumping and probing occur while the atom traverses the beam. In the wall-induced Ramsey effect, the atom travels about the cell undergoing many wall collisions before the probe interaction occurs. Thus the time between pumping and probing can be much longer for the wall-induced Ramsey effect compared to the transit effect, leading to the ultranarrow linewidths observed in the present work.

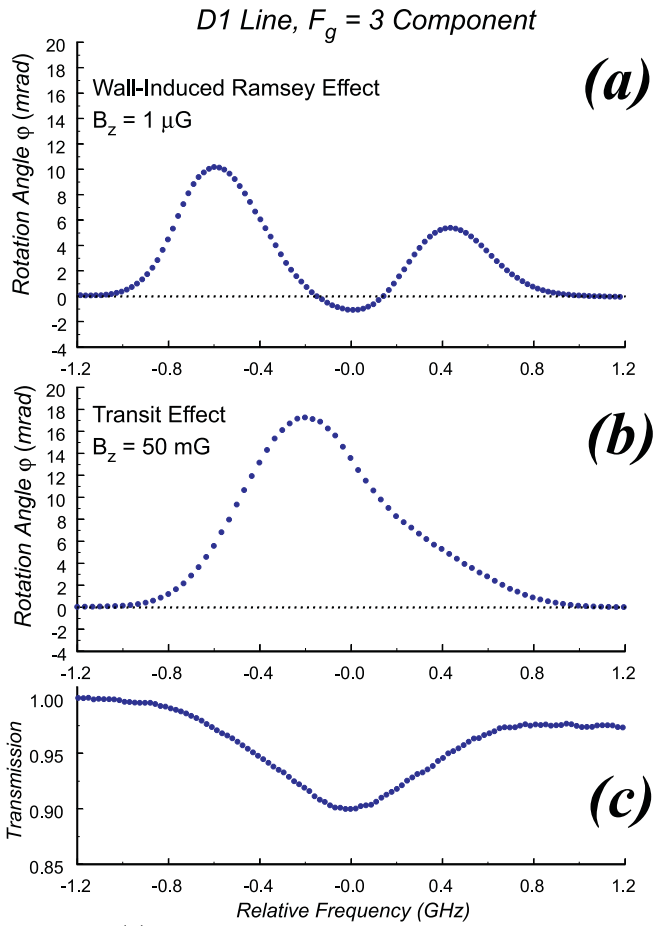

FIG. 4. (a) Wall-induced Ramsey rotation spectrum, light intensity is 1.2 mW/cm^2, beam diameter $\approx$ 3 mm. (b) Transit effect rotation spectrum, light intensity is 0.6 mW/cm^2. (c) Light transmission spectrum for light intensity = 1.2 mW/cm^2. Overall slope in light transmission is due to change in incident laser power during the frequency scan.

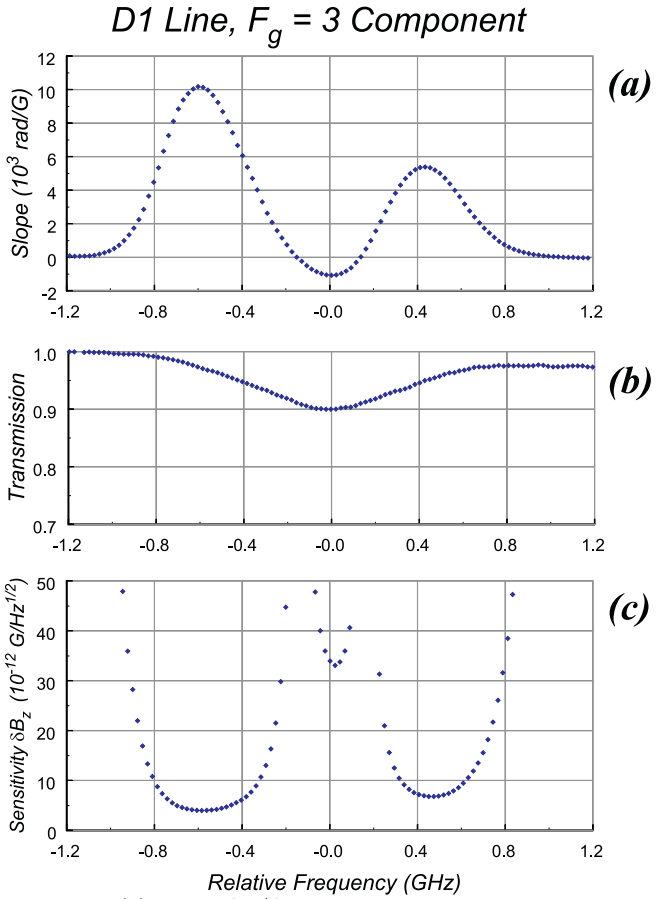

FIG. 5. (a) Slope $\partial\varphi/\partial B_z$ as a function of laser detuning for the $F_g = 3$ component of the Rb D1 line (laser intensity $\approx$ 1 mW/cm^2); (b) Normalized light transmission; (c) estimated shot-noise-limited sensitivity δB_z.

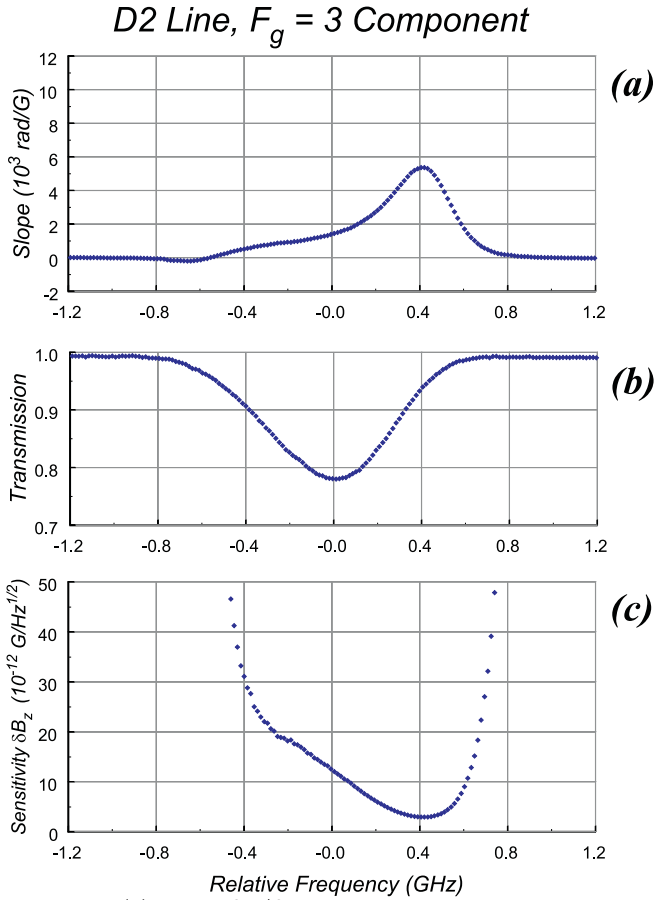

FIG. 6. (a) Slope $\partial\varphi/\partial B_z$ as a function of laser detuning for the $F_g = 3$ component of the Rb D2 line (laser intensity $\approx$ 4.5 mW/cm^2); (b) Normalized light transmission; (c) estimated shot-noise-limited sensitivity δB_z.

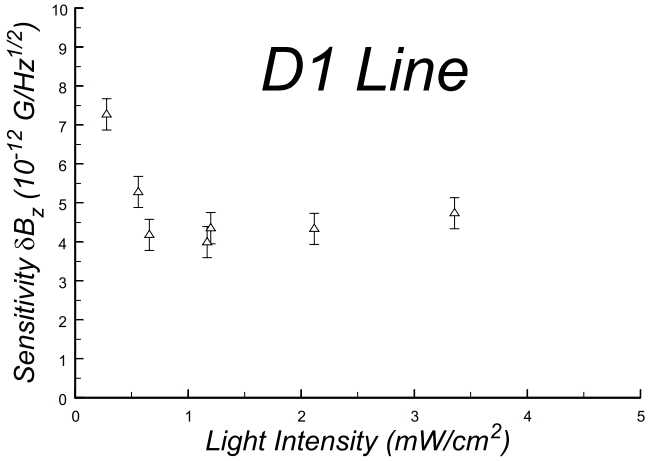

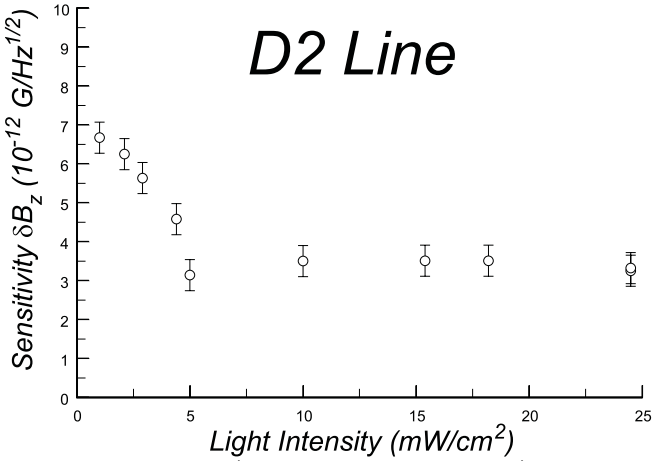

FIG. 7. Optimum (with respect to frequency) shot-noise-limited sensitivity as a function of light intensity for the $F_g = 3$ components of the D1 and D2 lines. Data taken at room temperature (20 ^{o}C, atomic density $\approx 4.5 \times 10^9$ cm^{-3}). Note that the scale of the horizontal axis is five times larger for the D2 line.

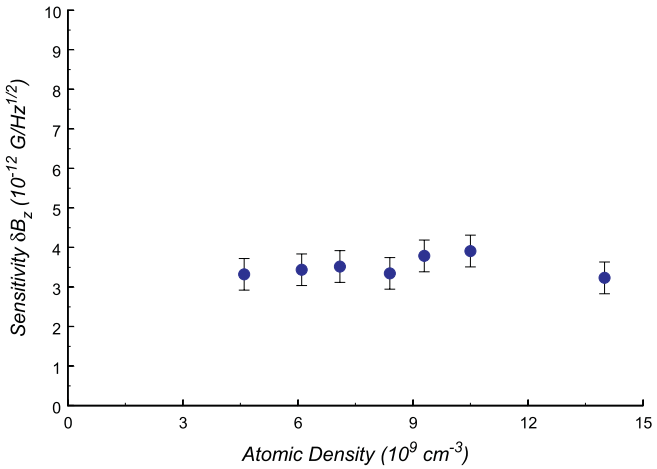

FIG. 8. Shot-noise-limited sensitivity as a function of atomic density for the $F_g = 3$ component of the D2 line, light intensity = 20 mW/cm^2. Light frequency at each point is chosen to achieve optimum sensitivity.